DOI: 10.1002/ejic.201100080

Formation and Reactivity of a Biomimetic Hydroperoxocopper(II) Cryptate

Laura Chaloner,[a] Mohammad S. Askari,[a] Adrian Kutteh,[a] Siegfried Schindler,[b] and Xavier Ottenwaelder*[a]

Keywords: Biomimetic complexes / Copper / Oxidation / Peroxides / Oxygen-atom transfer

Copper(II)-hydroperoxo species are proposed as key intermediates in the catalytic cycles of copper-monooxygenase enzymes that perform C–H bond hydroxylation. Herein we report on the oxidation chemistry of a copper(II) complex with a coordinating cryptand based on a peralkylated tetradentate tris(2-aminoethyl)amine (tren) moiety. X-ray crystallography of the copper(II) acetate complex of this cryptand revealed that the copper(II) ion is in a square-pyramidal environment, with the cryptand acting only as a tridentate ligand. This geometry is conserved in solution and likely results from restraints imposed by the semi-rigid cryptand. Reaction of this complex with basic hydrogen peroxide in methanol led to the decomposition of the complex with an oxygen-atom transfer to the ligand, as evidenced by mass spectrometry analysis after reaction and demetallation. Low-temperature stopped-flow experiments (down to –90 °C) support the formation of a copper(II)-hydroperoxo intermediate, CuOOH, before ligand oxygenation occurs. It is proposed that this intermediate performs the oxygen-atom transfer to a weak benzylic C–H bond of the cryptand, thereby mimicking the behavior of dopamine-β-hydroxylase.

Introduction

The ease with which enzymes perform oxidation reactions has long been coveted by synthetic chemists.[1] In this respect, copper monooxygenases are enzymes of particular interest because they can hydroxylate C–H bonds using low-toxicity copper as the key element.[2] Specifically, the enzyme peptidylglycine-α-hydroxylating monooxygenase (PHM) can hydroxylate a C–H bond in a glycine-extended peptide.[3] This enzyme activates dioxygen (O_2) at a mononuclear Cu^I ion (Cu_M) and performs insertion of one oxygen atom into the substrate with the assistance of a second mononuclear Cu^I ion (Cu_H) located at a distance of 11 Å from Cu_M. The enzyme dopamine-β-hydroxylase (DβH), which hydroxylates the benzylic position of dopamine, has a very similar active site to that of PHM.[4] The suggested mononuclear reaction intermediates involved in the C–H bond functionalization in these enzymes are the Cu^{II}-superoxo [Cu^{II}-($O_2^{\cdot-}$)], Cu^{II}-hydroperoxo [Cu^{II}-(OOH^-)], Cu^{III}-peroxo [Cu^{III}-(O_2^{2-})], and Cu^{II}-oxyl/Cu^{III}-oxo [Cu^{II}-($O^{\cdot-}$)/Cu^{III}-(O^{2-})] complexes.[5] A Cu^{II}-hydroperoxo species was first proposed as the active intermediate, but a Cu^{II}-superoxo species is now seen as a more likely culprit.[4–6] In particular, experimental evidence for the Cu^{II}-superoxo intermediate lies in the solid-state molecular structure of oxygenated crystals of PHM, in which the best structural fit at the active site is an end-on Cu^{II}-superoxo species.[3a]

Many synthetic efforts have been made to prepare and study reactive mononuclear Cu complexes that would be similar to the intermediates proposed in the enzymatic catalytic cycles.[1a,5b,7] Of interest to the present study are Cu^{II}-hydroperoxo species prepared using multidentate ligands. One such complex has been crystallographically characterized; it is supported by a tetradentate ligand that stabilizes the hydroperoxo group through hydrogen bonds.[8] This species shows little reactivity due to its stability. Because most Cu^{II}-hydroperoxo species are reactive, however, they are studied only in solution at low temperatures to prevent their decomposition. These species are thus characterized by spectroscopic means (UV/Vis features, resonance Raman, EPR).[9]

Herein we report oxidation studies on a Cu^{II} complex of a coordinating cryptand based on the tris(2-aminoethyl)amine (tren) ligand (Scheme 1); the peralkylated tren

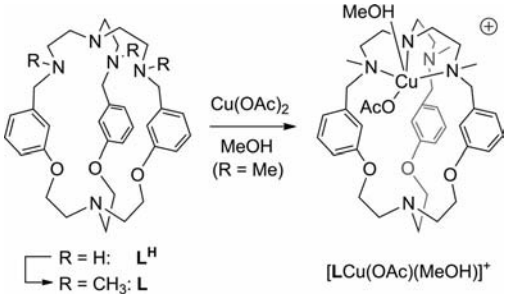

Scheme 1. Ligand **L** and preparation of its Cu^{II} acetate complex.

[a] Department of Chemistry and Biochemistry, Concordia University,
7141 Sherbrooke W, Montreal, QC, H4B 1R6, Canada
Fax: +1-514-848-2868
E-mail: xotten@alcor.concordia.ca
[b] Institut für Anorganische und Analytische Chemie, Justus Liebig Universität,
Heinrich-Buff-Ring 58, 35392 Gießen, Germany

moiety is well-known to support Cu/O_2 chemistry.[10] We were curious to study the effects of the semi-rigidity and the cavity of a cryptand on the reactivity of a Cu^{II}-hydroperoxo species given that second-sphere interactions are possible between the Cu^{II}-hydroperoxo species and the inside of the cryptand cavity. Such second-sphere interactions have been shown to be key factors in stabilizing reactive intermediates in metal–dioxygen chemistry.[8,11] In addition, the cryptand arms are based on benzyl linkers, which mimic the benzylic position that undergoes hydroxylation in the substrate of DβH.

Results and Discussion

The synthesis of the macrobicyclic ligand **L** involves *N*-methylation of the known cryptand $\mathbf{L^H}$.[12] Methylation was found to simplify the products deriving from the oxidation reactions carried out below; complexes of the non-methylated ligand $\mathbf{L^H}$ readily oxidized to imine compounds, thereby hampering the study of the oxygen-atom transfer reaction.[13] Slow diffusion of acetonitrile into a dichloromethane solution of **L** at –30 °C yielded single crystals that were amenable to X-ray diffraction analysis (Table 1). The molecular structure (Figure 1) indicates that the cryptand adopts an *endo-endo* conformation, as does its parent $\mathbf{L^H}$.[12a] The molecule displays an overall C_1 symmetry, notably due to the twist of the N4 arm of the tren moiety with one CH_2 (C19) inside the cavity. The bottom of the molecule displays three weak C–H···O contacts between the OCH_2 and the O atoms in the range 2.727–2.879 Å [van der Waals radii: $r_{vdW}(H)$ = 1.20 Å, $r_{vdW}(O)$ = 1.52 Å]. The molecule also wraps itself around weak C_{arom}–H···C_{arom} contacts between the aromatic groups [3.053–3.225 Å; $r_{vdW}(C)$ = 1.70 Å]. Lastly a triangular set of H···H contacts is observed between two benzylic CH_2 groups on the N2 and N5 atoms and the tren $N4CH_2$ group from the twisted arm (2.405–2.470 Å). Although very weak, these multiple interactions certainly exist to counteract the void that would be created by an open cavity and testify to a certain flexibility of the semi-rigid cryptand.

Table 1. Crystal data and details of structure determinations for **L** and [**L**Cu(OAc)(MeOH)](SbF$_6$).

	L	[**L**Cu(OAc)(MeOH)](SbF$_6$)
Empirical formula	$C_{36}H_{51}N_5O_3$	$C_{39}H_{58}CuF_6N_5O_6Sb$
Formula mass [g·mol^{-1}]	601.82	992.19
Color, habit	colorless, rod	blue, plate
Crystal dim. [mm]	0.40×0.10×0.10	0.10×0.08×0.04
Crystal system	orthorhombic	triclinic
Space group	$P2_12_12_1$	$P\bar{1}$
Z	4	2
a [Å]	13.2018(8)	11.4632(7)
b [Å]	13.5649(8)	13.0625(8)
c [Å]	18.4945(10)	14.8682(9)
α [°]	90	94.176(3)
β [°]	90	98.893(3)
γ [°]	90	104.495(2)
V [Å^3]	3312.0(3)	2115.0(2)
D_{calc} [mg·m^{-3}]	1.207	1.558
Radiation	Mo-K_α	Cu-K_α
Temperature [K]	110	150
θ range [°]	5.43–27.53	3.52–67.91
μ [mm^{-1}]	0.08	6.354
F(000)	1304	1018
Observed reflections	7109	33408
Independent reflections (R_{int})	4139 (0.024)	7533 (0.070)
Data/restraints/parameters	4139/0/400	7533/0/542
Goodness of fit on F^2	1.119	1.045
R indices (all data)	0.0423	0.0462
wR_2 indices [$I>2\sigma(I)$]	0.0854	0.1219
Largest diff. peak/hole [e·Å^{-3}]	0.23/–0.18	1.634/–1.049

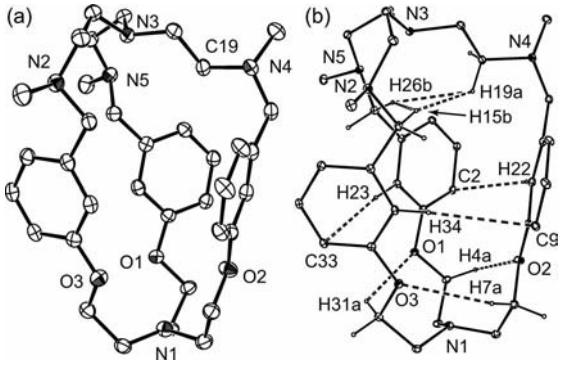

Figure 1. (a) ORTEP representation of **L** at 50% ellipsoid probability. Hydrogen atoms have been omitted for clarity. (b) ORTEP representation of **L** at 20% ellipsoid probability emphasizing the weak interatomic contacts (only selected hydrogens shown).

The binding of Cu^{II} to **L** was found to be highly dependent upon the choice of counterion. With BF_4^- or NO_3^- as counterions, the Cu^{II} complex did not form fully (incomplete coordination) in water, methanol, or ethanol, as indicated by a large residual ligand peak in the ESI-MS analysis. By contrast, the reaction of **L** with Cu^{II} acetate or formate in methanol or ethanol yielded a blue solution with only one ESI-MS peak corresponding to the complexes $[\mathbf{L}Cu(OAc)]^+$ or $[\mathbf{L}Cu(O_2CH)]^+$, respectively (Figure 2). With the $CF_3SO_3^-$ counterion, complexation only went to completion in an aprotic solvent such as THF; in protic solvents or in the presence of water or H_2O_2, the complex dissociated readily and the oxidation studies could not be conducted. Details on the oxidation studies that were performed on the acetate complex are given below.

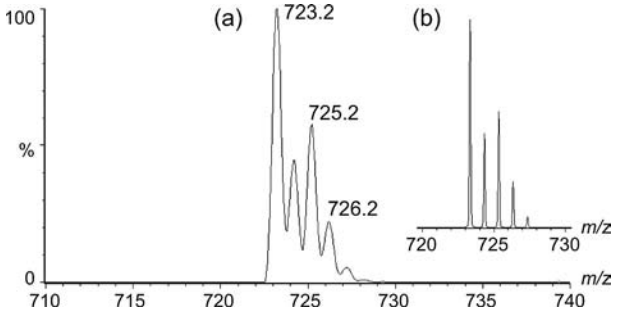

Figure 2. (a) ESI-MS of $[\mathbf{L}Cu(OAc)]^+$. (b) Predicted isotopic pattern of $[\mathbf{L}Cu(OAc)]^+$.

The acetate complex $[\mathbf{L}Cu(OAc)]^+$ was isolated and characterized in the solid state. By adding $NaSbF_6$ to a methanol solution of the acetate complex and allowing the solvent to evaporate, well-defined blue crystals of $[\mathbf{L}Cu(OAc)(MeOH)](SbF_6)$ formed within one hour. These crystals were studied by X-ray crystallography (Figure 3, Table 1). The structure of this complex displays several striking features. The Cu^{II} ion is coordinated by only three of the four nitrogen atoms of the tren moiety; the arm that is not coordinated (N4 arm) extends away from the metal ion. The square-pyramidal geometry of the Cu^{II} ion is completed by an acetate ion in the equatorial position *trans* to the central tren nitrogen atom (N1) and a methanol molecule at the apical position. Though slightly disordered at the methyl position, the methanol molecule is further involved in hydrogen bonding with the noncoordinated oxygen atom of the acetate ion (O2H···O6 2.583 Å). The square-pyramidal geometry of the metal ion could be the consequence of the semi-rigidity of the cryptand, but Cu^{II} complexes of ligand $\mathbf{L^H}$ with CN^-, SCN^-, and N_3^- ions adopt a distorted trigonal-bipyramidal geometry with all four nitrogen atoms of the tren moiety coordinated.[12a] In $[\mathbf{L}Cu(OAc)(MeOH)](SbF_6)$, the *N*-methyl groups, especially on N4 atom, may sterically hamper the cryptand to adopt a pseudo-C_3 conformation when the acetate anion is coordinated.

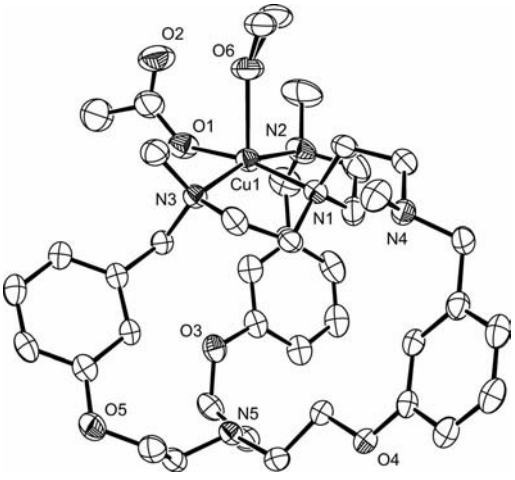

Figure 3. ORTEP drawing of $[\mathbf{L}Cu(OAc)(MeOH)](SbF_6)$ at 50% ellipsoid probability. The SbF_6^- counterion and hydrogen atoms have been omitted for clarity. Selected bond lengths [Å]: Cu1–O1 1.961(3); Cu1–O6 2.271(3); Cu1–N1 2.050(3); Cu1–N2 2.073(3); Cu1–N3 2.096(3).

The solution structure of the acetate complex was investigated by Electron Paramagnetic Resonance (EPR) spectroscopy. The EPR spectra, at 77 K, of a methanol solution formed by adding Cu^{II} acetate to **L** and that of dissolved $[\mathbf{L}Cu(OAc)(MeOH)](SbF_6)$ crystals in methanol both display an axial signal with $g_\parallel = 2.21$ ($A_\parallel = 180$ G) greater than $g_\perp = 2.03$, consistent with a $d(x^2 - y^2)^1$ electronic configuration. These spectra confirm the square-pyramidal geometry of the Cu^{II} ion in solution (for comparison, the aforementioned $\mathbf{L^H}$ complexes remain trigonal bipyramidal in solution).[12a] Coupled with the ESI-MS indicating a $[\mathbf{L}Cu(OAc)]^+$ formulation, this suggests that the acetate ion is still occupying an equatorial position of the Cu^{II} complex in methanol solution.

The $[\mathbf{L}Cu(OAc)]^+$ complex was reacted under the oxidative conditions commonly used to generate Cu^{II}-hydroperoxo species. The reaction of $[\mathbf{L}Cu(OAc)]^+$ with one equivalent of H_2O_2 and Et_3N in methanol was followed by UV/Vis spectroscopy between +20 and –60 °C. The reaction mixture gradually changed from blue to green but no band could be unambiguously assigned to the Cu^{II}-hydroperoxo species $[\mathbf{L}CuOOH]^+$, which is expected to display a hydroperoxo-to-Cu charge transfer around 380 nm ($\varepsilon \approx 900$–$1700\ M^{-1}cm^{-1}$).[8,9e,9h–9k] To study the oxidation process under more controlled conditions, the reaction was also carried out with 100 equivalents of H_2O_2 and Et_3N between –40 and –90 °C in a low-temperature stopped-flow spectrophotometer (Figure 4).[14] This increase in H_2O_2/Et_3N concentration led to a faster formation of an intermediate along a bimolecular pathway, which permitted its observation. The time-resolved spectral traces indicated a growth from the spectrum of $[\mathbf{L}Cu(OAc)]^+$ to that of a species with a distinct band shouldering around 380 nm and features in the visible range (Figure 4). This species then decayed in a slower process. Multivariate kinetic fitting of the growth using the Specfit software indicated a single exponential growth consistent with pseudo-first-order conditions. The fitting procedure revealed that the intermediate has absorptions at approximately 380 nm ($\varepsilon \approx 2000\ M^{-1}cm^{-1}$) and at 560 nm ($\varepsilon \approx 250\ M^{-1}cm^{-1}$), which are typical of the Cu^{II}-hydroperoxo species $[\mathbf{L}CuOOH]^+$.[8,9e,9h–9k] Fitting at several temperatures and Eyring analysis of the pseudo-first-order rate constants indicated that the growth process is associative with $\Delta H^\ddagger = 25.2\ kJ\,mol^{-1}$ and $\Delta S^\ddagger = -146\ J\ K^{-1}$

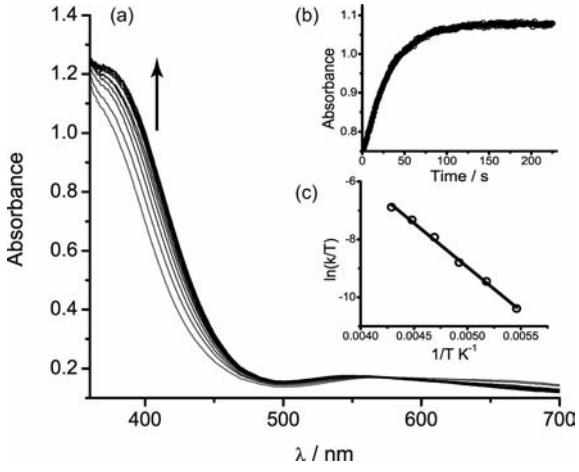

Figure 4. Stopped-flow UV/Vis spectroscopic studies of the reaction of $[\mathbf{L}Cu(OAc)]^+$ with 100 equiv. of a 1:1 H_2O_2/Et_3N mixture in MeOH at –70 °C; $[Cu]_{total} = 0.5$ mM after mixing. (a) Time-resolved absorption spectra for the first 450 s of the reaction; a spectrum is measured every 9 s; first spectrum at 4.5 s. (b) Growth profile at 395 nm with first-order fit. (c) Eyring plot from the pseudo-first-order rate constants measured at –90, –80, –70, –60, –50, and –40 °C: 5.66×10^{-3}, 1.55×10^{-2}, 3.07×10^{-2}, 7.72×10^{-2}, 0.147, and 0.238 s^{-1}, respectively (standard deviations from fitting within 1.4–3.7%).

mol^{-1} (Figure 4). No dimeric species [end-on or side-on peroxodicopper(II) and bis(μ-oxo)dicopper(III)][7a] were observed under any of the conditions used (concentration of H_2O_2/Et_3N, time of reaction). After being formed, the Cu^{II}-hydroperoxo complex decayed to a mixture of species with a relatively silent UV/Vis spectrum (Figure 5). Fitting the decay process between –40 °C and +20 °C, however, did not lead to a single consistent kinetic model, suggesting the involvement of more than a single step.

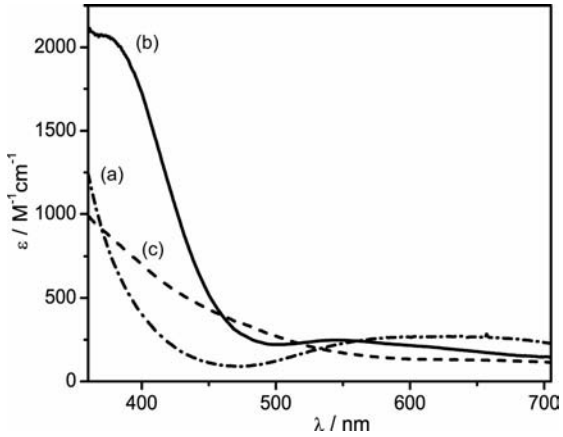

Figure 5. (a) UV/Vis spectra of [**L**Cu(OAc)]$^+$ at 20 °C. (b, c) UV/Vis spectra of the Cu^{II}-hydroperoxo intermediate (b, full) at –70 °C and the decay solution (c, dashed) at –40 °C deduced from stopped-flow measurements; in both cases the molar absorptivities were corrected from ca. 15 and 10% solvent contraction, respectively.

A comparison can be made between the present complex and the one studied by Itoh and co-workers in terms of the kinetics of formation and decay of the Cu-hydroperoxo intermediate.[14c,15] As is the case with [**L**Cu(OAc)]$^+$, Itoh's complex has an initial square-pyramidal geometry around the Cu center and it is believed that this geometry is conserved in their Cu-hydroperoxo intermediate. The second-order rate constants in Itoh's case fall in the range 4–5.1×10^4 M^{-1} s^{-1} at –90 °C. By comparison, [**L**Cu(OAc)]$^+$ is formed at a much slower rate, approximately 0.11 M^{-1} s^{-1} at –90 °C. This dramatic reduction in the rate of formation of the intermediate likely results from the steric demands and rigidity of the cryptand, which hamper substitution reactions in the Cu coordination sphere. Conversely, the cryptand-based intermediate decays qualitatively faster than Itoh's or other Cu^{II}-hydroperoxo intermediates. The rigidity of the cryptand is likely restricting movements of the arms that contain the sensitive CH bonds and this pre-arrangement is entropically beneficial for the oxygen-atom transfer step.

To decipher the nature of the reaction intermediates and products, ESI-MS experiments were carried out by using a continuous-flow mixing set-up. A 1 mM solution of [**L**Cu(OAc)]$^+$ and a 100 mM solution of H_2O_2/Et_3N were injected into coils that were cooled in a –85 °C bath. The solutions were mixed in a Y-junction immersed in the cold bath and the mixed solution then entered the ESI-MS instrument through a short capillary. As the injection flow rate was varied, different stages of the reaction were observed. The solutions were initially prepared in methanol, but due to the proximity in mass of methanol to two oxygen atoms, the spectra were more easily interpreted when the experiments were carried out in absolute ethanol. The MS data (Figure 6, a–c) revealed a complex mixture of species; putative assignments are listed in Table 2. As the reaction time was increased from approximately 1.5 to 6.3 then to 16 min, peaks corresponding to oxidized products increased in intensity. Unfortunately, due to the technical difficulty of keeping the entire length of the capillary containing the

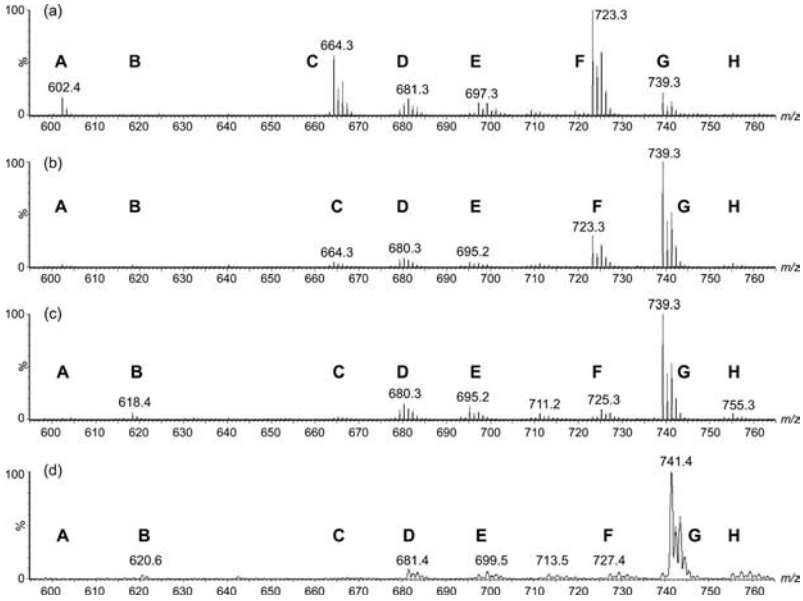

Figure 6. (a)–(c) ESI-MS of ethanol solutions of [**L**Cu(OAc)]$^+$ and H_2O_2/Et_3N mixed by continuous-flow methods at –85 °C prior to injection. The spectra were recorded after (a) 1.5, (b) 6.3, (c) 16 min of residence time after mixing. Assignments for groups A–H are given in Table 2. (d) ESI-MS of a [**L**Cu(OAc)]$^+$ solution reacted with $H_2{}^{18}O_2/Et_3N$ (5 equiv., –78 °C).

mixed solutions at very low temperature, and given the residence times prior to reaching the MS ionization chamber, it is unlikely that the intermediate was observed in this experiment as it decays fast at temperatures above –40 °C.

Table 2. Assignment of the main peaks in the low temperature continuous-flow MS experiments from Figure 6. The most relevant peaks are given in bold.

Position	*m/z*[a]	Assignment
A	**602**	$[\mathbf{L}]H^+$ (reactant)
B	**618**	$[\mathbf{L}+O]H^+$
C	**664**	$[\mathbf{L}+Cu]^+$
D	679	$[(\mathbf{L}+O-H)+Cu]^+$ (deprotonated hemiaminal)
	680	$[(\mathbf{L}+O)+Cu]^+$
	681	$[\mathbf{L}+Cu+OH]^+$
E	**695**	$[(\mathbf{L}+O-2H)+Cu+OH]^+$ (double oxidation)
	697	$[\mathbf{L}+Cu+OOH]^+$ or $[(\mathbf{L}+O)+Cu+OH]^+$
	699	$[\mathbf{L}+Cu+OH+OH_2]^+$
F	**723**	$[\mathbf{L}+Cu+OAc]^+$ (reactant)
	725	$[(\mathbf{L}+O-CH_2)+Cu+OAc]^+$ (double oxidation)
G	**739**	$[(\mathbf{L}+O)+Cu+OAc]^+$ (main product)
H	755	$[(\mathbf{L}+2O)+Cu+OAc]^+$ (double oxidation)

[a] These *m/z* ratios correspond to the position of the peak using isotopes ^1H, ^{12}C, ^{14}N, ^{16}O, and ^{63}Cu.

This ESI-MS experiment reveals the evolution of reactants and products upon reaction. Upon longer reaction times, the peaks corresponding to the starting material (F, C, and traces of free ligand A) decreased. Conversely, peaks assigned to oxidized products containing one extra oxygen atom increased in intensity upon longer reaction times, especially $[\mathbf{L}Cu(OAc)+O]^+$ (G; *m/z* = 739.3). One signal at *m/z* = 697.3 (in the E group) could correspond to the Cu^{II}-hydroperoxo species $[\mathbf{L}CuOOH]^+$, but it could also be due to a product in which the ligand is oxygenated $[(\mathbf{L}+O)CuOH]^+$, that is, the Cu^{II}-hydroxo complex of an oxygenated ligand (see below; for comparison, the Cu^{II}-hydroxo complex of **L** is found in D at *m/z* = 681.3, a peak that decreases with reaction time). As a note, a neutral $[\mathbf{L}Cu(OAc)(OOH)]$ complex could be the prevalent form of the intermediate observed by stopped-flow UV/Vis spectroscopy; the fact that this species would be MS-silent could explain the relatively small $[\mathbf{L}CuOOH]^+$ signal. Peaks assigned to overoxidized compounds are also observed and increase in intensity upon longer reaction times, but remain in small quantities. In particular, a peak at *m/z* = 695.2 could correspond to $[(\mathbf{L}+O-2H)+Cu+OH]^+$, that is, the Cu^{II}-hydroxo complex of a ligand that was doubly oxidized to either an amide or an aldehyde/imine (see below). Overall, however, the major product is the $[\mathbf{L}Cu(OAc)+O]^+$ species and it is concluded that the reaction is selective for monooxygenation despite the large excess of oxidant.

Isotopic labeling using ^{18}O-enriched hydrogen peroxide (from a solution in ^{16}O water) proved that the oxygen atom that is incorporated into the complex comes from the oxidant. When $H_2{}^{18}O_2$ was used {5 equiv. of $H_2{}^{18}O_2/Et_3N$ per $[\mathbf{L}Cu(OAc)]^+$}, the MS data displayed a peak at 741.4, which corresponds to $[\mathbf{L}Cu(OAc)+{}^{18}O]^+$, with a signal at 739.3 not significantly more intense than the 10% expected from the 90% isotopic enrichment of the oxidant (Figure 6, d). Thus, the entirety of the oxygen incorporated into the complex after reaction originated from H_2O_2 and this oxygen did not exchange with water in the timescale of the experiments (less than one hour).

To analyze the ligand modifications resulting from the oxidation reaction, demetalation was carried out by treatment with ammonium hydroxide or Na_4EDTA. The residual organic matter was then analyzed by ESI-MS. The cryptand nature of ligand **L** prevented much fragmentation and led to simple spectra with one major signal at *m/z* = 618.3 corresponding to $[\mathbf{L}+O]^+$, and some intact ligand at *m/z* = 602.3 (Figure 7, a). This experiment demonstrates the insertion of one oxygen atom into the ligand backbone and negligible amounts of double oxidation products, either as $[\mathbf{L}+2O]^+$, $[\mathbf{L}+O-2H]^+$, or $[\mathbf{L}-4H]^+$. As a control experiment, ligand **L** was treated with H_2O_2/Et_3N under the same conditions but no significant oxidation of the ligand occurred. Thus, the presence of Cu^{II} is essential to carry out the oxygenation reaction efficiently. In addition, when $H_2{}^{18}O_2$ was used, the oxygenated peak shifted to *m/z* = 620.4 for a $[\mathbf{L}+{}^{18}O]^+$ species (Figure 7, b), thereby confirming the incorporation of one oxygen atom from H_2O_2 into a non-exchangeable position of the ligand.

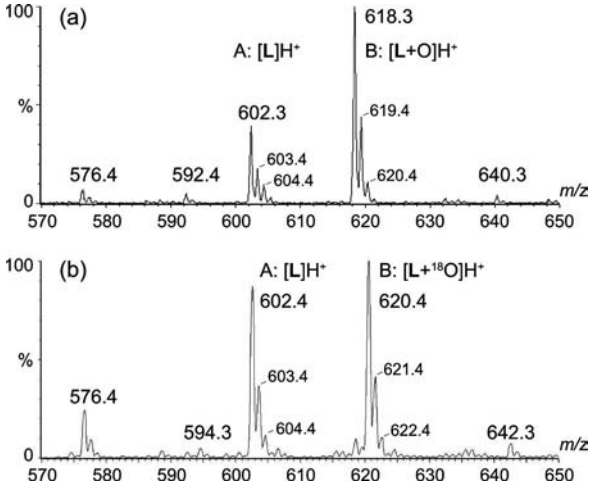

Figure 7. ESI-MS of the organic products of the oxidation reaction with (a) $H_2{}^{16}O_2$ and (b) $H_2{}^{18}O_2$ after demetallation, principally A = $[\mathbf{L}]H^+$ and B = $[\mathbf{L}+O]H^+$. The residual A signals arise because the reactions were stopped before completion. The A signals decrease when longer reaction times were used.

After demetalation, the solution contained several compounds (according to TLC, MS, and NMR spectroscopy) but we were unable to separate the compounds into their pure form for quantification purposes. This is likely the result of all products remaining as cryptands or macrocycles with structures close to that of the **L** precursor. Our best purification efforts using flash chromatography led to two impure fractions. The oxidized solution reacted with the Fuchsin-aldehyde reagent; the resulting aldehyde could clearly be seen after the reaction. This aldehyde was identified in the first fraction by ^1H NMR (well-defined peak at δ = 9.96 ppm in $CDCl_3$) and by solution IR spectroscopies (intense peak at 1708 cm^{-1}). The second fraction displayed

a weak peak at 1667 cm^{-1} in the IR spectrum, which is tentatively assigned to an amide. As the benzylic positions in **L** are the most sensitive ones to oxidation conditions, we propose that one of these positions is the target of the oxygen-atom transfer by the CuOOH intermediate. If oxygen-atom transfer had occurred to an *N*-methyl group, demethylation would occur together with the release of formaldehyde in solution. This pathway was not observed to be a major contributor to the reactivity of the complex (Table 2). Furthermore, a recent study involving $[Cu(Me_6tren)(OOH)]^+$ showed no decay reactivity of the intermediate with the permethylated tren ligand system.[10a]

Based on the above MS and UV/Vis analyses, we propose the reaction pathway shown in Scheme 2, which is inspired by the known reactivity of many Cu-dioxygen intermediates[7b] and Cu^{II}-hydroperoxo species.[9b,9d] This reaction pathway only accounts for the formation of the major $[\mathbf{L}Cu(OAc)+O]^+$ species observed by ESI-MS. The first step is the formation of a Cu^{II}-hydroperoxo species in an associative reaction between $[\mathbf{L}Cu(OAc)]^+$ and HOO^- generated in situ by deprotonation of H_2O_2.[14c,15] This intermediate was observed by UV/Vis spectroscopy but its proper formulation, geometry, and charge is yet unknown due to its relative instability. This intermediate then reacts with the benzylic position through an oxygen-atom transfer reaction akin to the current literature proposals for similar species,[9b,9j] thus producing a hemiaminal intermediate, which is deprotonated and bonded to Cu {*m*/*z* = 679 for $[(\mathbf{L}+O-H)+Cu]^+$} or protonated {*m*/*z* = 680 for $[(\mathbf{L}+O)+Cu]^+$ and *m*/*z* = 739 for $[(\mathbf{L}+O)+Cu+OAc]^+$}. Under the protic conditions used, this hemiaminal intermediate can readily hydrolyze to a secondary amine and an aldehyde (*m*/*z* = 739 as well), a functional group whose presence was confirmed in the decomposed mixture by both NMR and IR spectroscopies. Finally, minor products resulting from overoxidation could form through an intermolecular reaction of the hemiaminal with H_2O_2,[9b] intermolecular attack of HOO^- on an iminium intermediate (see below), or the complex of an already oxygenated ligand reentering the whole oxidation cycle.

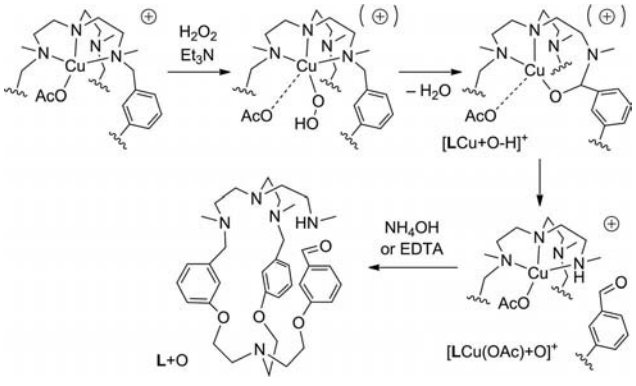

Scheme 2. Proposed reaction pathway for the inner-sphere oxidation reaction of $[\mathbf{L}Cu(OAc)]^+$ with H_2O_2/Et_3N. For clarity, the cryptand backbone has been simplified. The Cu^{II}-hydroperoxo complex (and other intermediates) may or may not be bonded to the acetate couterion, which would also influence the overall charge and their detection by ESI-MS.

The mechanism of the oxygen-atom transfer is still unknown but could proceed along two well-studied oxidative *N*-dealkylation pathways: a direct hydrogen-atom abstraction followed by rebound, or a single-electron transfer followed by further electron and proton transfers.[16] The hydrogen-atom abstraction mechanism entails hydrogen abstraction from the weak *N*-benzylic position by the electrophilic oxygen of the Cu^{II}-hydroperoxo complex to generate a carbon radical in the α position of the amine. Rebound of the putative Cu^{II}-oxyl species then produces the hemiaminal intermediate.[9b] The single-electron transfer mechanism, on the other hand, would generate an amine-based radical that can then lose a proton and an electron to form an iminium intermediate. Intramolecular nucleophilic attack of a coordinated oxo or hydroxo ion then leads to the same hemiaminal intermediate as above. Importantly, the hypothesis of an intermolecular attack of water onto the iminium intermediate has been refuted by ^{18}O isotopic labeling experiments. Thus, as per recent literature on oxygen-atom transfer reactions with Cu^{II}-hydroperoxo species, the hydrogen-atom abstraction mechanism seems to be the favored pathway.[9b,9j]

More studies are needed to substantiate the proposed reaction pathway of Scheme 2. In particular, ^{18}O isotopic labeling would be useful for measuring the O–O stretch of the Cu^{II}-hydroperoxo species by resonance Raman spectroscopy and to confirm its nature and involvement in the oxygenation reaction. Given the transient nature of this intermediate, however, excess $H_2{}^{18}O_2$ would be required for the intermediate to accumulate and be observed. Instead, we are currently trying to stabilize the intermediate by deuterating the oxidation-sensitive C–H bonds of the ligand (i.e., the benzylic positions and *N*-methyl substituents). This substitution would slow down the C–H activation step, which is thought to be rate determining (kinetic isotope effect). Increasing the oxidative stability of the ligand shall therefore lead to a Cu^{II}-hydroperoxo intermediate that can both be isolated at low-temperatures and reactive upon warming. This approach will facilitate the study of the electronic structure (by resonance Raman spectroscopy), the geometry (by EPR spectroscopy), and the reactivity of the intermediate.

Conclusion

The reaction between the Cu^{II}-cryptand complex $[\mathbf{L}Cu(OAc)]^+$ and H_2O_2/Et_3N leads to a single major oxygenated species upon oxygen-atom insertion into a weak C–H bond. Observation of a reactive intermediate in this reaction was achieved using pseudo-first-order conditions, very low temperatures and fast-mixing/recording stopped-flow techniques. The intermediate has the same UV/Vis spectroscopy and reactivity signatures as that of known Cu^{II}-hydroperoxo species,[5b,9j] which strongly suggests that the reaction involves such a Cu^{II}-hydroperoxo species borne

by the cryptand. It is not yet known whether the hydroperoxo group is encapsulated by the cavity of the cryptand and thereby supported by second coordination sphere interactions. Whereas the crystal structure of the acetate complex suggests that *N*-methylation prevents the cryptand from adopting a pseudo-C_3 symmetry once coordinated, the coordination geometry could change upon binding the smaller and more linear hydroperoxide anion. A correlation indeed exists between coordination geometry and anion size in cryptand complexes.[17] Further studies are in progress to render the ligand less sensitive to oxidation and stabilize the intermediate species to enable a more complete characterization.

Experimental Section

General: All materials were used as received. The synthesis of ligand $\mathbf{L^H}$ has been reported elsewhere.[12a] NMR spectroscopic measurements were made at 22 °C in a 5 mm tube on a Varian Innova 300 or 500 MHz instrument and referenced to internal TMS. ESI-MS spectra were measured using direct injection on a Micromass Q-TOF or a Micromass Quattro LC at Concordia's Centre for Biological Applications of Mass Spectrometry. The *m*/*z* data reported are based on ^{1}H, ^{12}C, ^{14}N, ^{16}O, and ^{63}Cu. X-ray crystallography was performed on the molybdenum source of a Bruker APEX DUO (**L**) or the copper rotating anode source of a Bruker Microstar {[**L**Cu(OAc)(MeOH)](SbF$_6$)}. UV/Vis spectra were recorded on an Agilent 8453 spectrophotometer equipped with a Unisoku USP-203-A cryostat for temperatures down to –60 °C.

Ligand L: $\mathbf{L^H}$ (1.00 g, 1.8 mmol) was added to a solution of formaldehyde (740 μL, 10.6 mmol) and formic acid (400 μL, 10.6 mmol). The mixture was heated under reflux for 24 h. The solution was cooled and was poured onto an aqueous solution of NaOH (30 mL; 2 M). The product was extracted with dichloromethane (3 × 20 mL) and the organic phase extracts were dried with anhydrous Na_2SO_4. The solvent was removed under reduced pressure, yielding a precipitate that was suspended in acetonitrile. Filtration, washing with acetonitrile, and drying under vacuum yielded 0.82 g (76%) of a white powder. Single crystals amenable to X-ray diffraction analysis were grown by the slow diffusion of acetonitrile into a dichloromethane solution of **L** at –30 °C (Table 1). ^1H NMR (300 MHz, $CDCl_3$): δ = 2.15 (s, 9 H, CH_3), 2.32 (t, 6 H, CH_2), 2.59 (t, 6 H, CH_2), 3.08 (t, 6 H, CH_2), 3.31 (s, 6 H, CH_2), 4.04 (t, 6 H, CH_2), 6.67 (m, 3 H, Ar), 6.73 (m, 3 H, Ar), 7.00 (s, 3 H, Ar), 7.11 (m, 3 H, Ar) ppm. ^{13}C NMR (300 MHz, $CDCl_3$): δ = 43.4 (CH_3), 52.5 (CH_2), 54.5 (CH_2), 57.4 (CH_2), 62.8 (CH_2), 68.9 (CH_2), 114.7 (Ar), 114.8 (Ar), 121.5 (Ar), 129.0 (Ar), 141.0 (Ar), 159.4 (Ar) ppm. MS (ESI, 1:1 CH_3OH/CH_2Cl_2): *m*/*z* = 602.41 $[M + H]^+$.

[LCu(OAc)(MeOH)]$^+$ Solutions and [LCu(OAc)(MeOH)](SbF$_6$) Crystals: A solution of copper(II) acetate (8.0 mg, 39 μmol) dissolved in methanol (800 μL) was added to a solution of **L** (24 mg, 39 μmol) dissolved in dichloromethane (200 μL). The solution was used as is for further experiments (100% formation as evidenced by a single ESI-MS signal at *m*/*z* = 723.31). Single crystals were grown by the addition of $NaSbF_6$ (1 equiv.) dissolved in the minimum amount of methanol to a solution of the complex in methanol and allowing the solution to stand for 1 h (Table 1).

Bulk Oxidation Studies: A methanol solution (1 equiv.) of H_2O_2/Et_3N (1:1; the H_2O_2 was from a 30 wt.-% aqueous solution) was added to a methanol solution of [**L**Cu(OAc)(MeOH)]$^+$ (1.0 mM) at –78 °C turning the solution green. After 10 min, the solution was warmed to room temperature and analyzed by ESI-MS. Whether the reaction was performed under an air or nitrogen atmosphere did not change the kinetics, colors, and products.

Isotopic Labeling Experiments: A methanol solution (5 equiv.) of $H_2{}^{18}O_2$/Et_3N (1:1; the $H_2{}^{18}O_2$ came from a 2.5 wt.-% solution in $H_2{}^{16}O$) was added to a methanol solution of [**L**Cu(OAc)]$^+$ (1.0 mM) at –78 °C and the resulting solution turned green. After 10 min, the solution was warmed to room temperature and analyzed by ESI-MS.

Analysis of Organics: After decomposition of the oxidized reaction mixture, excess NH_4OH or Na_4EDTA was added and the solution was filtered through an alumina column eluted with 20% MeOH in CH_2Cl_2. The filtrate was analyzed by ESI-MS. Our attempts to isolate pure oxygenated products from the mixture were unsuccessful.

Kinetic Measurements: Kinetic studies of the reaction of H_2O_2/Et_3N with [**L**Cu(OAc)]$^+$ were recorded on a modified Hi Tech SF-3 L low-temperature stopped-flow unit (Salisbury, UK) equipped with a J&M TIDAS 16-500 diode array spectrophotometer (J&M, Aalen, Germany).[14a,14b,18] Complex solutions before mixing were 1.0 mM and the concentration of the H_2O_2/Et_3N mixture was 100 mM to ensure pseudo-first-order conditions and help the formation of the intermediate before it could decay. The reaction was studied at temperatures between +20 and –90 °C. Complete spectra were collected with the integrated J&M software Kinspec 2.30 and analyzed with a global analysis fitting routine using the program Specfit (Spectrum Software Associates, Chapel Hill, USA).

CCDC-808560 (for **L**) and -795492 {for [**L**Cu(OAc)(MeOH)](SbF$_6$)} contain supplementary crystallographic data. These data can be obtained free of charge from The Cambridge Crystallographic Data Centre via www.ccdc.cam.ac.uk/data_request/cif.

Acknowledgments

This work was supported by grants from the Fonds de Recherche sur la Nature et les Technologies of Quebec (FQRNT) and the Natural Sciences and Engineering Research Council of Canada (NSERC). S. S. gratefully acknowledges financial support from the Deutsche Forschungsgemeinschaft (DFG) (SPP1118 and SCHI377/6-2). We are grateful to Francine Bélanger-Gariépy (Université de Montréal) for X-ray crystallography studies on [**L**Cu(OAc)](SbF$_6$), to Frank Schaper (Université de Montréal) for access to his Specfit software, and to Scott Bohle (McGill University) for recording the EPR spectra. M. S. A. acknowledges NSERC for CGS-M and PGS-D scholarships and a Michael Smith Foreign Study Supplements award.

[1] a) L. Que, W. B. Tolman, *Nature* **2008**, *455*, 333–340; b) W. B. Tolman (Ed.), *Biomimetic Oxidations Catalyzed by Transition Metal Complexes*, Imperial College Press, London, **2000**.
[2] E. I. Solomon, U. M. Sundaram, T. E. Machonkin, *Chem. Rev.* **1996**, *96*, 2563–2606.
[3] a) S. T. Prigge, B. A. Eipper, R. E. Mains, L. M. Amzel, *Science* **2004**, *304*, 864–867; b) S. T. Prigge, R. E. Mains, B. A. Eipper, L. M. Amzel, *Cell Mol. Life Sci.* **2000**, *57*, 1236–1259; c) A. T. Bauman, E. T. Yukl, K. Alkevich, A. L. McCormack, N. J. Blackburn, *J. Biol. Chem.* **2006**, *281*, 4190–4198.
[4] J. P. Klinman, *J. Biol. Chem.* **2006**, *281*, 3013–3016.
[5] a) E. I. Solomon, J. W. Ginsbach, D. E. Heppner, M. T. Kieber-Emmons, C. H. Kjaergaard, P. J. Smeets, L. Tian, J. S. Woertink, *J. Chem. Soc. Faraday Trans.* **2011**, *148*, 11–39; b) S. Itoh,

Curr. Opin. Chem. Biol. **2006**, *10*, 115–122; c) M. Rolff, F. Tuczek, *Angew. Chem.* **2008**, *120*, 2378; *Angew. Chem. Int. Ed.* **2008**, *47*, 2344–2347; d) R. A. Himes, K. D. Karlin, *Curr. Opin. Chem. Biol.* **2009**, *13*, 119–131.

[6] a) P. Chen, E. I. Solomon, *J. Am. Chem. Soc.* **2004**, *126*, 4991–5000; b) P. Chen, E. I. Solomon, *Proc. Natl. Acad. Sci. USA* **2004**, *101*, 13105–13110; c) A. Decker, E. I. Solomon, *Curr. Opin. Chem. Biol.* **2005**, *9*, 152–163; d) A. Crespo, M. A. Martí, A. E. Roitberg, L. M. Amzel, D. A. Estrin, *J. Am. Chem. Soc.* **2006**, *128*, 12817–12828; e) T. Kamachi, N. Kihara, Y. Shiota, K. Yoshizawa, *Inorg. Chem.* **2005**, *44*, 4226–4236.

[7] a) L. M. Mirica, X. Ottenwaelder, T. D. P. Stack, *Chem. Rev.* **2004**, *104*, 1013–1046; b) E. A. Lewis, W. B. Tolman, *Chem. Rev.* **2004**, *104*, 1047–1076; c) C. J. Cramer, W. B. Tolman, *Acc. Chem. Res.* **2007**, *40*, 601–608; d) P. J. Donoghue, A. K. Gupta, D. W. Boyce, C. J. Cramer, W. B. Tolman, *J. Am. Chem. Soc.* **2010**, *132*, 15869–15871; e) A. Kunishita, M. Kubo, H. Sugimoto, T. Ogura, K. Sato, T. Takui, S. Itoh, *J. Am. Chem. Soc.* **2009**, *131*, 2788–2789; f) C. Würtele, E. Gaoutchenova, K. Harms, M. C. Holthausen, J. Sundermeyer, S. Schindler, *Angew. Chem.* **2006**, *118*, 3951; *Angew. Chem. Int. Ed.* **2006**, *45*, 3867–3869; g) D. Maiti, D.-H. Lee, K. Gaoutchenova, C. Würtele, M. C. Holthausen, A. A. Narducci Sarjeant, J. Sundermeyer, S. Schindler, K. D. Karlin, *Angew. Chem.* **2008**, *120*, 88; *Angew. Chem. Int. Ed.* **2008**, *47*, 82–85; h) J. S. Woertink, L. Tian, D. Maiti, H. R. Lucas, R. A. Himes, K. D. Karlin, F. Neese, C. Würtele, M. C. Holthausen, E. Bill, J. Sundermeyer, S. Schindler, E. I. Solomon, *Inorg. Chem.* **2010**, *49*, 9450–9459; i) D. Maiti, H. C. Fry, J. S. Woertink, M. A. Vance, E. I. Solomon, K. D. Karlin, *J. Am. Chem. Soc.* **2007**, *129*, 264–265; j) G. Izzet, J. Zeitouny, H. Akdas-Killig, Y. Frapart, S. Menage, B. Douziech, I. Jabin, Y. Le Mest, O. Reinaud, *J. Am. Chem. Soc.* **2008**, *130*, 9514–9523; k) G. Thiabaud, G. Guillemot, I. Schmitz-Afonso, B. Colasson, O. Reinaud, *Angew. Chem.* **2009**, *121*, 7519; *Angew. Chem. Int. Ed.* **2009**, *48*, 7383–7386; l) A. K. Gupta, W. B. Tolman, *Inorg. Chem.* **2010**, *49*, 3531–3539.

[8] A. Wada, M. Harata, K. Hasegawa, K. Jitsukawa, H. Masuda, M. Mukai, T. Kitagawa, H. Einaga, *Angew. Chem.* **1998**, *110*, 874; *Angew. Chem. Int. Ed.* **1998**, *37*, 798–799.

[9] a) A. Kunishita, J. D. Scanlon, H. Ishimaru, K. Honda, T. Ogura, M. Suzuki, C. J. Cramer, S. Itoh, *Inorg. Chem.* **2008**, *47*, 8222–8232; b) D. Maiti, A. A. Narducci Sarjeant, K. D. Karlin, *Inorg. Chem.* **2008**, *47*, 8736–8747; c) A. Kunishita, M. Kubo, H. Ishimaru, T. Ogura, H. Sugimoto, S. Itoh, *Inorg. Chem.* **2008**, *47*, 12032–12039; d) D. Maiti, A. A. Narducci Sarjeant, K. D. Karlin, *J. Am. Chem. Soc.* **2007**, *129*, 6720–6721; e) D. Maiti, H. R. Lucas, A. A. Narducci Sarjeant, K. D. Karlin, *J. Am. Chem. Soc.* **2007**, *129*, 6998–6999; f) M. Kodera, T. Kita, I. Miura, N. Nakayama, T. Kawata, K. Kano, S. Hirota, *J. Am. Chem. Soc.* **2001**, *123*, 7715–7716; g) T. Ohta, T. Tachiyama, K. Yoshizawa, T. Yamabe, T. Uchida, T. Kitagawa, *Inorg. Chem.* **2000**, *39*, 4358–4369; h) S. Yamaguchi, A. Wada, S. Nagatomo, T. Kitagawa, K. Jitsukawa, H. Masuda, *Chem. Lett.* **2004**, *33*, 1556–1557; i) S. Yamaguchi, S. Nagatomo, T. Kitagawa, Y. Funahashi, T. Ozawa, K. Jitsukawa, H. Masuda, *Inorg. Chem.* **2003**, *42*, 6968–6970; j) Y. Syuhei, M. Hideki, *Sci. Technol. Adv. Mater.* **2005**, *6*, 34; k) T. Fujii, A. Naito, S. Yamaguchi, A. Wada, Y. Funahashi, K. Jitsukawa, S. Nagatomo, T. Kitagawa, H. Masuda, *Chem. Commun.* **2003**, 2700–2701.

[10] a) Y. J. Choi, K.-B. Cho, M. Kubo, T. Ogura, K. D. Karlin, J. Cho, W. Nam, *Dalton Trans.* **2011**, *40*, 2234–2241; b) S. Schindler, *Eur. J. Inorg. Chem.* **2000**, 2311–2326; c) C. Würtele, O. Sander, V. Lutz, T. Waitz, F. Tuczek, S. Schindler, *J. Am. Chem. Soc.* **2009**, *131*, 7544–7545.

[11] R. L. Shook, A. S. Borovik, *Inorg. Chem.* **2010**, *49*, 3646–3660.

[12] a) D. K. Chand, P. K. Bharadwaj, *Inorg. Chem.* **1996**, *35*, 3380–3387; b) A. P. Cole, V. Mahadevan, L. M. Mirica, X. Ottenwaelder, T. D. P. Stack, *Inorg. Chem.* **2005**, *44*, 7345–7364.

[13] A. De la Lande, O. Parisel, H. Gérard, V. Moliner, O. Reinaud, *Chem. Eur. J.* **2008**, *14*, 6465–6473.

[14] a) M. Weitzer, M. Schatz, F. Hampel, F. W. Heinemann, S. Schindler, *J. Chem. Soc., Dalton Trans.* **2002**, 686–694; b) M. Weitzer, S. Schindler, G. Brehm, S. Schneider, E. Hörmann, B. Jung, S. Kaderli, A. D. Zuberbühler, *Inorg. Chem.* **2003**, *42*, 1800–1806; c) T. Osako, S. Nagatomo, Y. Tachi, T. Kitagawa, S. Itoh, *Angew. Chem.* **2002**, *114*, 4501; *Angew. Chem. Int. Ed.* **2002**, *41*, 4325–4328.

[15] T. Osako, S. Nagatomo, T. Kitagawa, C. Cramer, S. Itoh, *J. Biol. Inorg. Chem.* **2005**, *10*, 581–590.

[16] B. Chiavarino, R. Cipollini, M. E. Crestoni, S. Fornarini, F. Lanucara, A. Lapi, *J. Am. Chem. Soc.* **2008**, *130*, 3208–3217.

[17] P. Mateus, R. Delgado, P. Brandão, V. Félix, *Chem. Eur. J.* **2011**, *17*, 7020–7031.

[18] L. Westerheide, F. K. Müller, R. Than, B. Krebs, J. Dietrich, S. Schindler, *Inorg. Chem.* **2001**, *40*, 1951–1961.

Received: January 24, 2011
Published Online: August 12, 2011

